Bioelectronic Tongue Using Heterodimeric Human Taste Receptor for the Discrimination of Sweeteners with Human-like Performance

Hyun Seok Song,[†,#] Hye Jun Jin,[‡,#] Sae Ryun Ahn,[†] Daesan Kim,[§] Sang Hun Lee,[†] Un-Kyung Kim,[⊥] Christopher T. Simons,[∥] Seunghun Hong,[‡,*] and Tai Hyun Park[†,¶,*]

[†]School of Chemical and Biological Engineering, Bio-MAX Institute, [‡]Department of Physics and Astronomy, and Institute of Applied Physics, and [§]Department of Biophysics and Chemical Biology, Seoul National University, Seoul, 151-747, Republic of Korea, [⊥]Department of Biology, Kyungpook National University, Daegu 702-701, Republic of Korea, [∥]Department of Food Science & Technology, The Ohio State University, Columbus, Ohio 43210-1007, United States, and [¶]Advanced Institutes of Convergence Technology, Suwon 443-270, Republic of Korea. [#]These authors contributed equally to this work.

ABSTRACT The sense of taste helps humans to obtain information and form a picture of the world by recognizing chemicals in their environments. Over the past decade, large advances have been made in understanding the mechanisms of taste detection and mimicking its capability using artificial sensor devices. However, the detection capability of previous artificial taste sensors has been far inferior to that of animal tongues, in terms of its sensitivity and selectivity. Herein, we developed a bioelectronic tongue using heterodimeric human sweet taste receptors for the detection and discrimination of sweeteners with human-like performance, where single-walled carbon nanotube field-effect transistors were functionalized with nanovesicles containing human sweet taste receptors and used to detect the binding of sweeteners to the taste receptors. The receptors are heterodimeric G-protein-coupled receptors (GPCRs) composed of human taste receptor type 1 member 2 (hTAS1R2) and human taste receptor type 1 member 3 (hTAS1R3), which have multiple binding sites and allow a human tongue-like broad selectivity for the detection of sweeteners. This nanovesicle-based bioelectronic tongue can be a powerful tool for the detection of sweeteners as an alternative to labor-intensive and time-consuming cell-based assays and the sensory evaluation panels used in the food and beverage industry. Furthermore, this study also allows the artificial sensor to exam the functional activity of dimeric GPCRs.

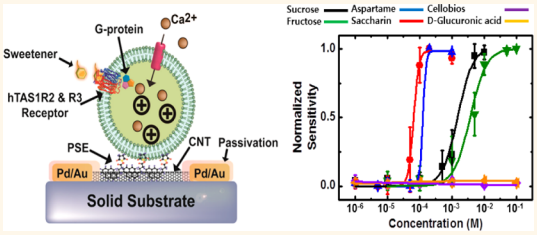

KEYWORDS: bioelectronic tongue · human sweet taste receptor · heterodimeric G-protein-coupled receptor · single-walled carbon nanotube · nanovesicle

Artificial taste sensors such as electronic tongues have been extensively studied, due to their broad applications in the food and beverage industry.[1,2] For example, the electronic tongues usually utilize synthetic materials such as polymers, semiconductors, or lipid membranes in the form of an array to detect known tastants.[3−6] Even with technical advances, most previous artificial sensors could not mimic the natural features of a human taste system in regards the specific recognition of tastant molecules in complex mixtures such as food and drinks. On the other hand, mammalian taste receptors allow for the identification of various taste molecules that evoke sensations typically referred to as sweet, bitter, salty, sour, and umami. For example, human sweet taste receptor proteins specifically bind to sweet compounds including sucrose, glucose, aspartame, and saccharin.[7,8] This property allows humans to recognize both nutritive and non-nutritive forms of sweeteners.[9,10] Thus, the use of human taste receptor proteins, belonging to the family of G-protein-coupled receptors (GPCRs), has been suggested for use as the sensing material to best mimic the human taste system.[9−15] Our previous studies, using a lipid membrane including a human *bitter* taste receptor as a recognition element, suggested that taste receptor proteins can be applied to the development of human-like bioelectronic

* Address correspondence to thpark@snu.ac.kr, seunghun@snu.ac.kr.

Received for review May 29, 2014 and accepted August 15, 2014.

Published online August 15, 2014
10.1021/nn502926x

tongues.[14,15] However, unlike the *bitter* taste receptor composed of a *single* protein component, the mammalian *sweet* taste receptor is a *heterodimeric* class C GPCR composed of *two* different proteins, hTAS1R2 and hTAS1R3.[7,10] hTAS1R2 and hTAS1R3 each have different functional roles and multiple ligand binding sites, and the proteins have to form a single combined receptor unit to recognize diverse sweeteners.[7,8,10] Until now, it has been extremely difficult, if not impossible, to combine them as a part of man-made functional devices for practical applications, which has been a major hurdle in building versatile functional devices such as sweet taste sensors.

GPCRs are involved in important physiological functions including neurotransmitter and hormone signaling.[16,17] Some GPCRs including sweet taste receptors are required to form homodimers or heterodimers for roles such as specific recognition of a ligand, agonist-induced activation, and downstream signaling.[18−20] Despite the importance of *dimeric* GPCRs for the improvement of new pharmaceuticals and drug therapies, the conventional methods using biochemical, biophysical, and functional complementation techniques have been limited by time-consuming procedures and low signal-to-noise ratios.[21−23]

Herein, we fabricated single-walled carbon nanotube field-effect transistor (swCNT-FET)-based artificial sweet taste sensors for the human-like detection and discrimination of sweeteners through hybridization with nanovesicles containing human taste receptors, heterodimeric GPCRs composed of hTAS1R2 and hTAS1R3. The nanovesicle-based bioelectronic tongues (NBTs) recognized various sweeteners including natural and artificial sweeteners with high sensitivity and human-like broad selectivity. Using swCNT-FET sensor platforms and heterodimeric sweet taste receptor-expressed nanovesicles, the sweet taste receptor-mediated signal transductions in nanovesicles were efficiently monitored. This study is the first demonstration of the artificial taste sensor utilizing heterodimeric human sweet taste receptors as recognition elements and mimicking human-like broad selectivity for the detection of various sweet tastants that have different chemical structures. Furthermore, our NBTs open up the opportunity to develop facile and reproducible methods to study the functional activity of *dimeric* GPCRs using our nanosensor platforms.

RESULTS AND DISCUSSION

Fabrication of Nanovesicle-Based Bioelectronic Tongues Containing Human Sweet Taste Receptors, Heterodimeric GPCRs. Figure 1 shows the schematic diagram representing the fabrication method of NBT devices. Briefly, the HEK-293 cells were transfected with a mammalian expression vector containing the hTAS1R3 gene, and the cells stably expressing hTAS1R3 were selected by using antibiotics. Then, hTAS1R3-expressed HEK-293 cell lines were transfected with a mammalian expression vector containing the hTAS1R2 gene. As a result, we could obtain HEK-293 cells expressing the human sweet taste receptor composed of hTAS1R2 and hTAS1R3. The coexpressed hTAS1R2 and hTAS1R3 in HEK-293 cells functioned as heterodimeric human sweet taste receptors which have multiple ligand binding sites for sweeteners.[7,8,10] These cells were then treated with cytochalasin B, which destroyed the cytoskeleton to make the cell membrane unstable. With gentle agitation, nanovesicles containing sweet taste receptors were budded out from the hTAS1R2/hTAS1R3-expressing HEK-293 cells. These nanovesicles contain sweet taste receptors and the cell signaling machinery including the G protein, adenylyl cyclase, and ion channels (Figure 1a). swCNT-FETs for NBTs were fabricated following the method reported previously.[24,25] The swCNT-FETs were then treated with linker molecules, pyrenebutyric acid *N*-hydroxysuccinimide ester (PSE) (Figure 1b). The pyrenyl groups in PSE interacted with the basal plane of graphite at the sidewall of swCNTs *via* π-stacking.[26] The nanovesicles containing sweet taste receptors were then immobilized on the PSE-functionalized swCNT-FETs through peptide bonds. Our advanced technique for the large-scale fabrication of the swCNT sensor platform allowed the production of a cost-effective nanovesicle-immobilized swCNT sensor chip.

Expression of Heterodimeric Human Sweet Taste Receptors and Construction of Nanovesicles. The stable expression of hTAS1R3 in HEK-293 was confirmed from the membrane fractions of HEK-293 cells by Western blot analysis, using antiflag antibody against flag-tag fused with hTAS1R3 (Figure 2a). The 95 and 180 kDa bands represent the monomeric and dimeric forms of the receptor protein, respectively. It was reported that GPCRs and other integral membrane proteins form dimers and larger oligomers even under the denaturation conditions for SDS-PAGE.[27] The formation of multimers is thought to be caused by nonspecific aggregation resulting from the formation of spurious disulfide bonds. After the construction of stable cell lines expressing hTAS1R3, these cell lines were transiently transfected with the hTAS1R2 gene fused with green fluorescence protein (GFP) to induce the heterodimer of hTAS1R2 and hTAS1R3. We confirmed the expression of hTAS1R2 in HEK-293 cells by fluorescence microscopy (Figure 2b). Green fluorescence was observed from the stable hTAS1R3 HEK-293 cell line transfected with hTAS1R2-GFP. These results indicate that the human sweet taste receptor composed of hTAS1R2 and hTAS1R3 was successfully expressed in HEK-293 cells.

To investigate whether intracellular signal transduction occurred in sweet taste cells, Ca^{2+} influx was measured through a transient calcium signal assay (Figure 2c). Ca^{2+} influx was measured by the calcium indicator Fura2-AM in HEK-293 cells expressing the

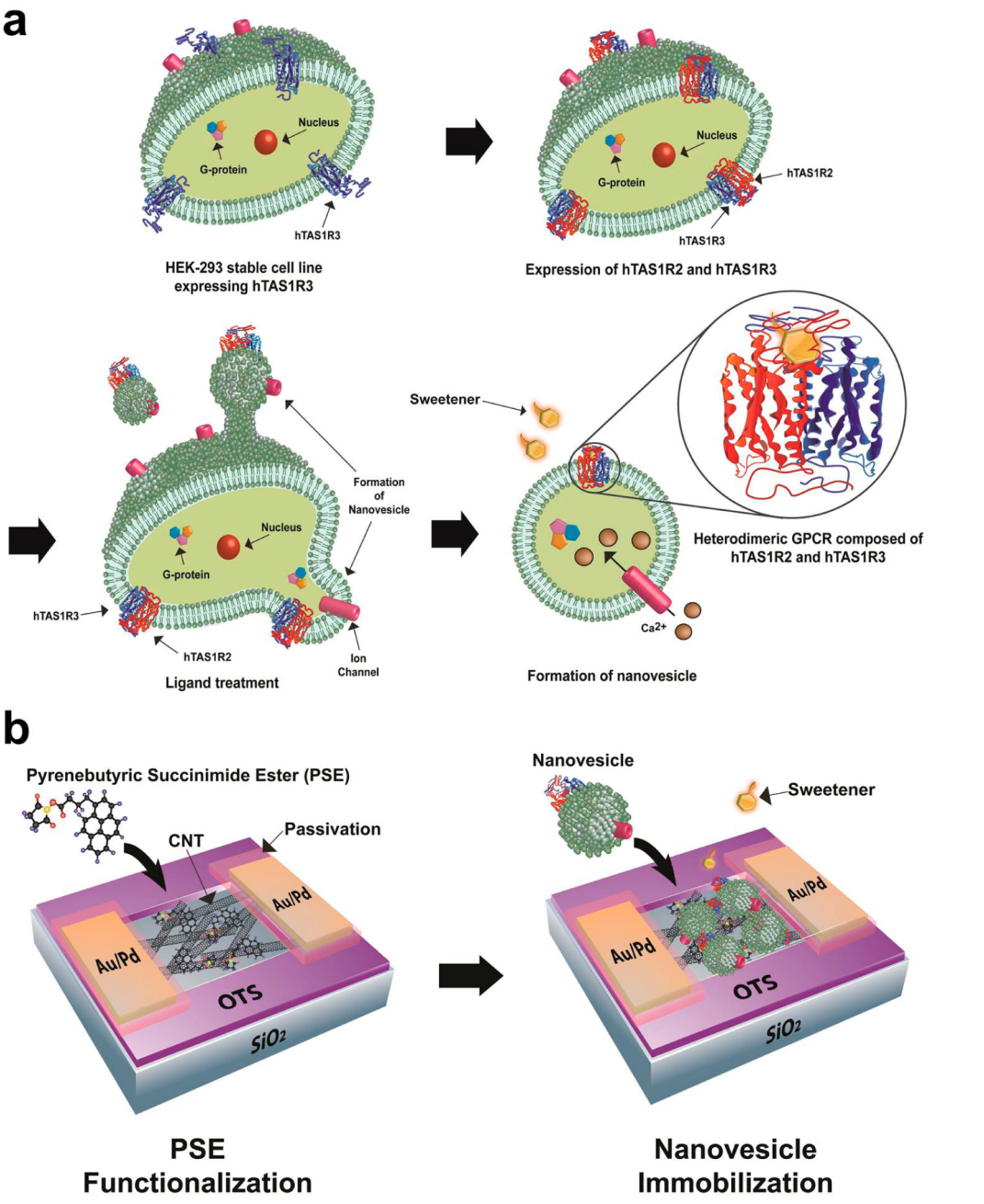

Figure 1. Schematic diagram depicting the fabrication procedure of sweet taste sensors using nanovesicles containing heterodimeric human sweet taste receptors. (a) Preparation of nanovesicles containing heterodimerinc GPCRs composed of hTAS1R2 and hTAS1R3 from HEK-293 cells. A stable HEK-293 cell line expressing hTAS1R3 was constructed, and hTAS1R2 was transiently expressed. This resulted in the expression of sweet taste receptors, composed of hTAS1R2 and hTAS1R3. The formation of nanovesicles containing human taste receptors was carried out with cytochalasin B treatment and a gentle agitation. The nanovesicles contained heterodimeric GPCRs composed of hTAS1R2 and hTAS1R3, human sweet taste receptors, and intracellular second messenger systems needed for taste sensory signal transduction. Therefore, nanovesicles could selectively respond to sweeteners *via* complete cell-like human taste receptor-mediated signal transduction. (b) Hybridization of the nanovesicles with a sensor transducer based on a swCNT-FET. The CNT-based sensor transducer was coated with PSE for the stable immobilization of nanovesicles *via* amide bonding.

human sweet taste receptor upon the injection of the sweetener, sucrose. Note that the addition of sucrose (10 mM) to hTAS1R2- and hTAS1R3-expressing cells induced the immediate increase in the fluorescence ratio (ratio of the fluorescence at 340 and 380 nm). It is known that the increase of intracellular Ca^{2+} concentration results from the binding event between the sweet taste receptor and sweetener.[9,10] This result shows that the intracellular signal transduction in sweet taste cells was efficiently mediated after the binding of sucrose to the human sweet taste receptors.

Western blotting was carried out to confirm whether cell-derived nanovesicles contain an efficient amount of receptors (Figure 2d). The thick bands at

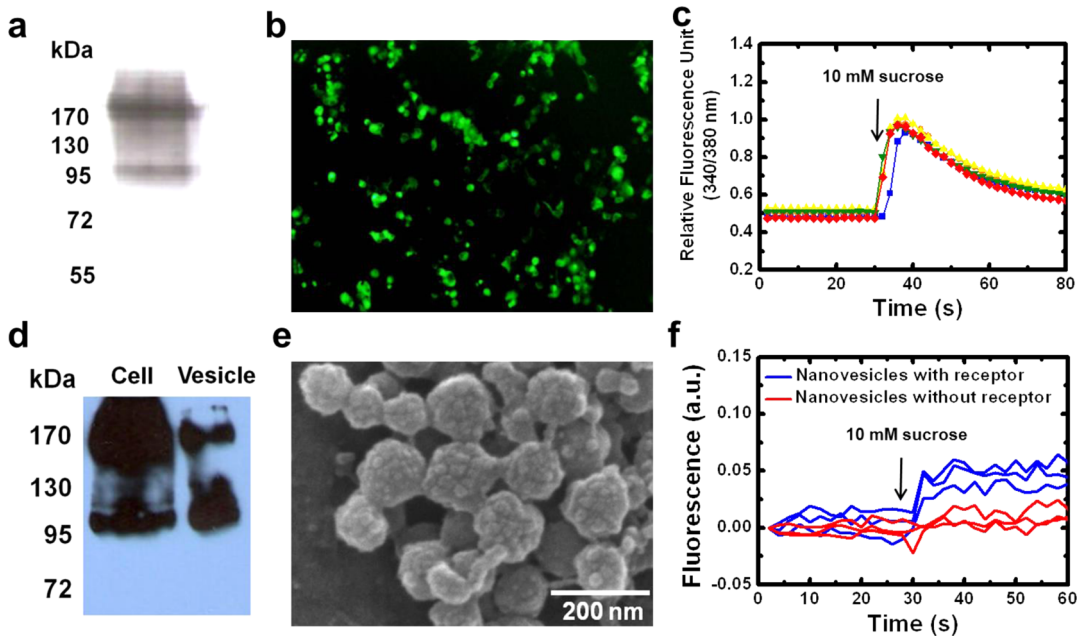

Figure 2. Construction of hTAS1R2/hTAS1R3-incorporated cells and nanovesicles. (a) Western blot analysis of TAS1R3 stably expressed in the HEK-293 cell membrane. (b) Fluorescence image of GFP-tagged hTAS1R2 expressed in the hTAS1R3 stable cell line. (c) Ca^{2+} signal analysis using hTAS1R2/hTAS1R3-expressed cells upon the addition of 10 mM of sucrose. A calcium influx was induced by sucrose, the ligand of hTAS1R2/hTAS1R3, and then Fura2 dyes emitted fluorescence by binding with calcium ions. (d) Western blot analysis of human sweet taste receptors in the cells and nanovesicles derived from the cells. (e) FE-SEM image of nanovesicles. (f) Ca^{2+} signal analysis using hTAS1R2/hTAS1R3-containing nanovesicles upon the addition of 10 mM of sucrose.

95 and 180 kDa represent the monomeric and dimeric forms of the receptor protein, respectively, found from both the membrane fraction of cells and the nanovesicles. By comparing thickness of each band found from the cell and nanovesicle fractions, we determined that the nanovesicles produced by our method contain a sufficient amount of taste receptors.

The formation and size distribution of nanovesicles were investigated by field-emission scanning electron microscopy (FE-SEM) (Figure 2e). The nanovesicles exhibited a well-defined spherical shape with diameters of 100−200 nm. Nanovesicles were also analyzed by dynamic light scattering (DLS) for the measurement of their size distribution (Figure S1 in Supporting Information). The DLS analysis result shows the uniform size of nanovesicles at 100−200 nm on average. This indicates that we successfully produced nanovesicles with a uniform size and a well-defined shape.

After the construction of nanovesicles from the HEK-293 cells expressing human sweet taste receptors, an intracellular calcium image analysis was carried out to investigate whether sweet taste receptor-mediated intracellular signals could also occur in the nanovesicles (Figure 2f). Here, the nanovesicles contained the calcium ion indicator, Fura2-AM, and the real-time calcium influx into the nanovesicles was monitored using a fluorescence microscope. The intensity of fluorescence increased upon sucrose stimulation, showing that a sweet taste receptor-mediated signal was generated. This indicates that nanovesicles can mimic the human sweet taste signal transduction. However, the restoration of the Ca^{2+} signal to the baseline was not observed, whereas signals obtained from whole cell experiments showed the recovery to the baseline following cessation of sucrose stimulation. A plausible explanation is that the nanovesicles lacked ion pumps and calmodulines which were required to restore the Ca^{2+} concentration.[28,29]

Characterization and Detection of Sucrose with Sweet Taste Nanovesicle-Based Bioelectronic Tongues. The detection mechanism of our NBT device is shown in Figure 3a. The binding event between the sweet taste receptor and sweeteners triggered signal transduction inside the nanovesicles through G proteins, adenylyl cyclase, and ion channels. Finally, the Ca^{2+} influx resulted from the signal transduction. This increase of Ca^{2+} concentration in nanovesicles gave a positive field effect on the underlying swCNT channel which had the p-type behavior (Figure S2 in Supporting Information). Therefore, the specific binding of sweeteners to sweet taste receptors could be detected by measuring the conductance change of the swCNT-FET. In previous studies, ligand−receptor binding was detected through the direct measurement of charge states of the receptors using swCNT-FETs.[15,30,31] However, our device indirectly detected the binding between sweeteners and sweet taste receptors by the measurement of accumulating charges in nanovesicles triggered by the signal.[24,25,32] This is closer to the mechanism

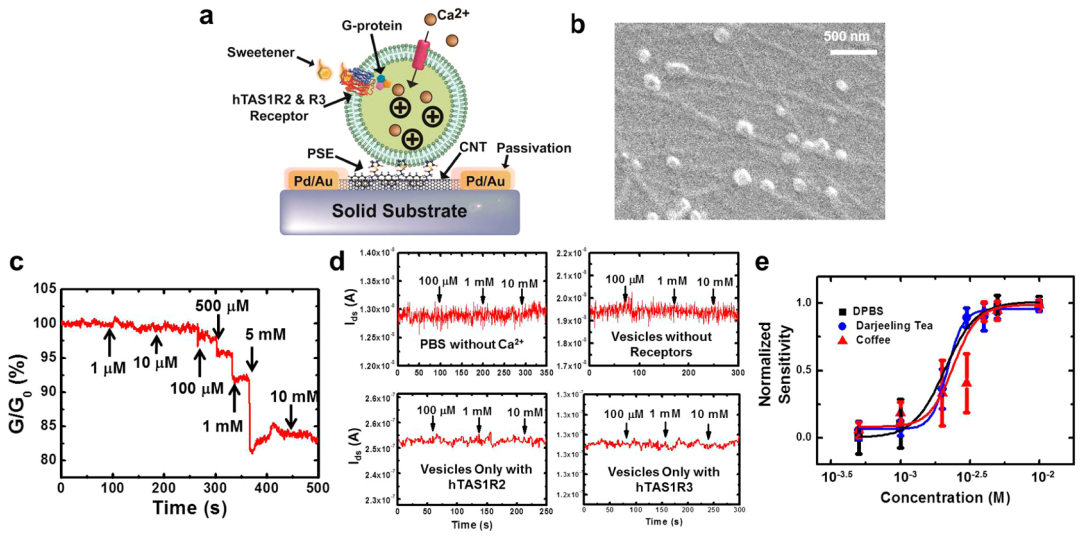

Figure 3. Detection of sucrose with nanovesicle-based bioelectronic tongues. (a) Schematic diagram depicting the sensing mechanism of a NBT. (b) SEM image of nanovesicles immobilized on swCNT networks. (c) Real-time conductance measurement data obtained from a NBT after the introduction of sucrose. The conductance began to decrease after the introduction of a sucrose solution with a 500 μM concentration. (d) Real-time responses of NBTs to various concentrations of sucrose under different conditions including nanovesicles in PBS without Ca^{2+}, nanovesicles without sweet taste receptors, and nanovesicles only with either hTAS1R2 or hTAS1R3. (e) Dose-dependent responses of NBTs to sucrose in DBPS, Darjeeling tea, and coffee.

underpinning human taste receptor-expressed cells compared to previous protein-based bioelectronic sensors and may mimic the human sweet taste system more closely.

Figure 3b shows the FE-SEM image of nanovesicles immobilized on a swCNT channel. The FE-SEM image was obtained after the lyophilization of the nanovesicle–swCNT surface and Pt coating on it. The image clearly shows the spherical-shaped nanovesicles on the line-shaped swCNTs. The immobilized nanovesicles had rather uniform sizes of ~100 nm. It should be mentioned that nanovesicles actually had a larger diameter before immobilization (Figure 2e). This is likely due to the use of different buffers after the immobilization of nanovesicles.

Figure 3c shows the real-time response of a NBT to sucrose. The source–drain currents of the NBT were monitored using a semiconducting analyzer (Keithley 4200), upon stimulation with a sucrose solution. The sensor began to show an immediate response to sucrose at a concentration of 500 μM. On the other hand, the conductance change was saturated at around 5 mM of sucrose. Furthermore, control experiments were carried out to investigate various factors related to sweetener detection (Figure 3d). First, the response from the NBT to sucrose was measured in PBS without Ca^{2+}. Second, sucrose responses were measured from a NBT containing nanovesicles constructed from wild-type HEK-293 cells expressing no sweet taste receptors. Third, responses were measure from nanovesicles that only contain hTAS1R2 and hTAS1R3 separately. In all control experiments, no signal changes from the NBTs were observed following stimulation with sucrose. These results clearly show that sweet taste receptors and Ca^{2+} ions are essential components for the response of the NBT, and heterodimeric structures composed of hTAS1R2 and hTAS1R3 are required for the sweet taste signal transduction. In addition, these negative control experiments support the detection mechanism.

Figure 3e shows the normalized sensitivity of the NBT to different concentrations of sucrose in Dulbecco's phosphate buffered saline (DPBS), Darjeeling tea, and coffee. Sample preparation is described in the Materials and Methods section. Note that the normalized sensor sensitivity increased as the concentration of sucrose increased, and it saturated at a high concentration region. Significantly, the responses of NBTs to sucrose in a DPBS solution and different drink samples exhibited similar characteristics. These results indicate that the NBT could measure sucrose concentrations even in complicated environments such as various drinks.

The dose-dependent response of the NBT was analyzed by fitting the experimental data with the model based on the Hill equation as reported previously (solid lines).[15,24] If we assume that binding characteristics between receptors and sweeteners followed the Hill equation model, the density C_s of sweetener bound to the receptor can be written as

$$C_s = \frac{C_{s,max} \cdot C^n}{1/K^n + C^n} \quad (1)$$

Here, C and K represent the concentration of sweetener in a solution and an equilibrium constant between a sweetener and a receptor, respectively. $C_{s,max}$ is the

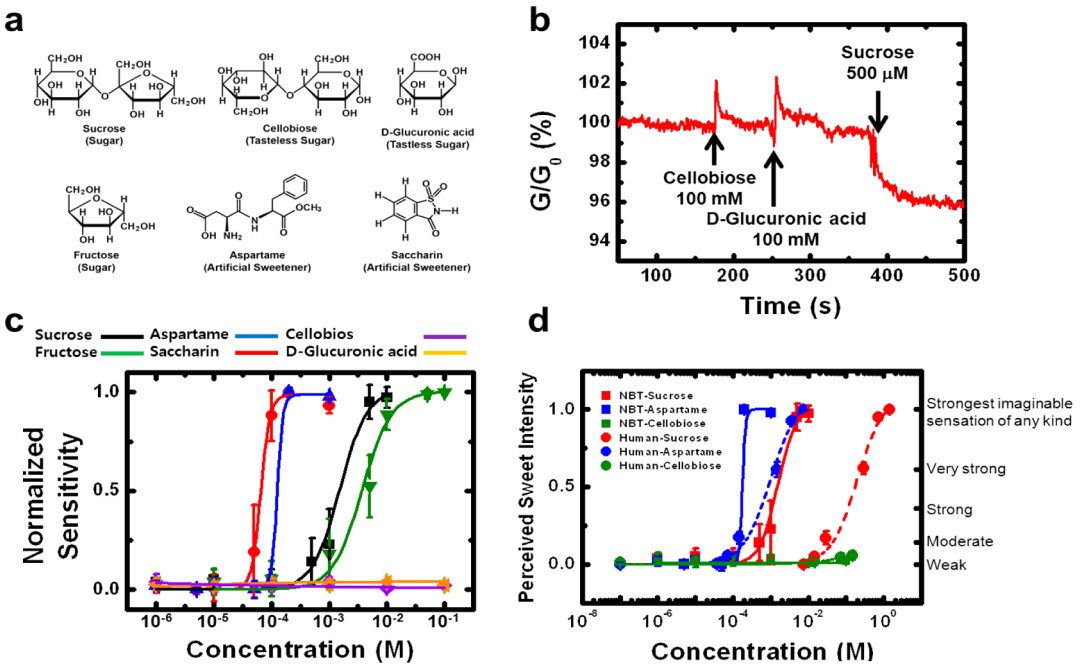

Figure 4. Human tongue-like discrimination of various sweeteners using nanovesicle-based bioelectronic tongues. (a) Chemical structures of various sweeteners. (b) Real-time response showing the human tongue-like selectivity of a NBT. The addition of 100 mM tasteless sugars (cellobiose and D-glucuronic acid) did not induce a sensor response, whereas the addition of a 500 μM sucrose solution caused a decrease in the conductance of the NBT device. (c) Dose-dependent response of NBTs to various sweet sugars (natural sweeteners), artificial sweeteners, and tasteless sugars. The artificial sweeteners showed lower equilibrium constants compared to that of natural sweeteners, indicating that the artificial sweeteners were a more potent agonist than natural sweeteners. (d) Sweet-evoked responses by NBTs and a sensory evaluation. Subjects evaluated aqueous solutions of sucrose, aspartame, and cellobiose. The normalized sensitivity of NBTs and the perceived sweet intensities of human sensation increased as the concentration of sucrose and aspartame increased. Both NBT devices and humans responded to substantially lower concentrations of an artificial sweetener (aspartame) compared to natural sweetener (sucrose). On the other hand, cellobiose elicited only a very weak sweet sensation at the highest concentration tested in both cases. These results indicate that the responses of the NBT to tastants are similar to those of the human taste system in terms of broad selectivity.

concentration of receptors on the swCNT-FET, and n is the Hill coefficient. If we assume that a conductance change ΔG is approximately proportional linearly to the number of bound sweetener molecules, a sensor sensitivity $|G/G_0|$ can be approximated as $|G/G_0| \sim kC_s$, where k is a constant representing the response characteristics of the NBT sensor. The sensor sensitivity converges to the maximum value of $k \times C_{s,max}$ as C becomes very large. Thus, the normalized sensitivity N can be written as

$$N = \frac{C^n}{1/K^n + C^n} \qquad (2)$$

By fitting the data in Figure 3d using eq 2, the equilibrium constants K between sucrose and the NTBs could be estimated. Interestingly, the estimated K values in DPBS and various drinks were all $\sim 2.0 \times 10^{-3}$ M, which clearly shows that our NBT could be utilized to detect and monitor sweeteners in real drink samples.

Human Tongue-like Selectivity for Sweetener Detection. We carried out extensive experiments to verify the human tongue-like broad selectivity for the detection of sweeteners. Figure 4a shows the chemical structures of various tastants for the selectivity test. The real-time response of the NBT to various sugars such as sucrose, cellobiose, and D-glucoronic acid is shown in Figure 4b. The addition of sucrose (500 μM) elicited a decrease in the current of ~5%, while no significant current changes occurred following stimulation with much higher concentrations (100 mM) of the tasteless sugars, cellobiose and D-glucoronic acid. Although, these sweet tastants have different chemical structures and sizes, our NBT could discriminate with broad selectivity. This indicates that the NBT shows human-like selective responses to sweeteners.

Figure 4c shows the normalized sensitivity of the NBT at different concentrations of various tastants. The normalized sensor sensitivity increased as the concentrations of sweeteners increased, and it saturated at a high concentration region. On the other hand, there were no significant normalized sensitivity changes upon the addition of tasteless sugars. Here, the dose-dependent responses of NBTs to sweet sugars (natural sweeteners) and artificial sweeteners followed the Hill equation model. Interestingly, the NBT showed more sensitive responses to artificial sweeteners (aspartame and saccharin) than to natural sweeteners (sucrose and fructose), indicating that artificial sweeteners were more potent agonists than natural sweeteners.

The results indicate that the NBT exhibited broad selectivity as previous cell-based functional assays using the human sweet taste receptor.[10,33] On the other hand, in terms of its sensitivity, the NBT responded to the lower concentration of the sweeteners than living cells did. Presumably, since nanovesicles were much smaller than living cells, the small amount of ion influx into the nanovesicles could significantly enhance their electrical potential, which enabled the detection of sweeteners at very low concentrations.[24] These features heighten the potential utility of the NBT in basic research on the human taste system as well as in applications such as artificial tongues which are important in the food and beverage industry.[5,6]

We performed sensory evaluation studies to compare responses from our NBT to human sensation. Figure 4d shows normalized responses of our NBT (solid line) and human sensory responses (dashed line) to sucrose, aspartame, or cellobiose. Sensory trials were completed in which subjects rated perceived intensity over large concentration ranges of sucrose, aspartame, or cellobiose. Similar to our NBT behavior, human sensory responses to sucrose and aspartame increased significantly at concentrations above threshold and plateaued once a saturating level of sweetness was perceived (red and blue trace, respectively). This compares to the weak sweet sensation elicited by cellobiose only at the highest concentration tested (green trace). The concentrations needed to evoke sweet sensations in human trials were expectedly higher than those needed to elicit nanovesicle responses. This is not surprising given the small size of the nanovesicle and, hence, the small ion influx needed to enhance the electrical potential. Similarly, in the nanovesicle-based assay, sweet compounds have direct access to taste receptors expressed on the external face of the plasma membrane. In contrast, with human trials, sweet compounds are diluted by the presence of saliva and must access taste receptors through taste pores that are often plugged with mucous. Nonetheless, the similarity of dose–response curves strongly suggests that nanovesicles containing human sweet taste receptors are able to recapitulate the human sensation. Therefore, the utilization of nanovesicles containing human sweet taste receptors allowed a human-like broad selectivity for the detection of sweeteners. These characteristics for mimicking the human sensation are unique compared to previous artificial taste sensors.[4,34–37]

CONCLUSION

The human tongue-like NBT was successfully developed using swCNT-FETs and nanovesicles containing human taste receptors composed of heterodimeric class C GPCRs as sensing and recognition elements, respectively. The sweetener sensor NBT recognized various sweeteners including natural and artificial sweeteners with high sensitivity and human-like broad selectivity. Using a swCNT-FET sensor platform, the sweet taste receptor-mediated signal transduction in nanovesicles was efficiently monitored. This strategy enabled a biosensor with human-like broad selectivity for the detection of sweeteners. This strategy can be used to overcome the limitations of conventional artificial tongues in terms of its sensitivity and selectivity and for various practical applications in the food and beverage industry. Also, this study offers a useful tool for the basic functional study of dimeric GPCRs. We also would like to point out that this device has the possibility to substitute for labor-intensive and time-consuming cell-based functional assays and human sensory trials used for the screening of taste receptors and tastants.

MATERIALS AND METHODS

Construction of HEK-293 Stable Cell Line Expressing hTAS1R2 and hTAS1R3. Human embryonic kidney-293 (HEK-293) cells were cultured in Dulbecco's modified Eagle medium (DMEM) supplemented with 10% fetal bovine serum and 0.5% penicillin–streptomycin (Gibco) at 37 °C under 5% CO_2. Cells were transfected with the mammalian expression vector, pCMV6-ENTRY, containing hTAS1R3, using Lipofectamine 2000 (Invitrogen) according to the manufacturer's instructions. After the transfection, cells were cultured for 1 day with the same condition mentioned above and transferred to the media containing G-418 (1 mg/mL) for selection. After the transferred cells were cultured for a week, G-418-resistant cell colonies were separately picked up and cultured in fresh media containing G-418. The stable expression of hTAS1R3 on the cell membrane was confirmed by Western blot analysis. The stable HEK-293 cell line expressing hTAS1R3 was transfected with pCMV6-GFP-hTAS1R2 by using Lipofectamine 2000 (Invitrogen). After the transfection, the expression of hTAS1R2-GFP was confirmed by monitoring the green fluorescence from GFP fused at the C-terminus of hTAS1R2.

Construction of Nanovesicles from HEK-293 Expressing Human Sweet Taste Receptor. Suspended HEK-293 cells expressing human sweet taste receptors in DMEM containing cytochalasin B (20 μg/mL) were incubated at 37 °C with 300 rpm agitation. Cells and cell debris were separated by centrifugation at 2000*g* for 30 min, and nanovesicles were collected by centrifugation at 12 000*g*. The nanovesicles were suspended in PBS containing a protease inhibitor cocktail (Sigma). Produced nanovesicles were used immediately or stored at −80 °C for the subsequent experiments.

Western Blot Analysis. All samples including the membrane fraction of cells and nanovesicles were mixed with SDS sample buffer (10% sodium dodecyl sulfate, 10% β-mercaptoethanol, 0.3 M Tris-HCl (pH 6.8), 0.05% bromophenol blue, 50% glycerol) and boiled for 5 min. The same amount of sample was loaded onto 10% PAGE gels (Laemmli) and electrophoresed at 80 V. Proteins in the gel were transferred to a nitrocellulose membrane. To enhance the selective binding of antibodies, the membrane was incubated with 5% skim milk in PBS-T (PBS containing 0.1% Tween-20) for 2 h. Antiflag antibody solution (from mouse, 1:1000 dilution with 1% skim milk in PBS-T) was applied to the blocked membrane and incubated at room temperature for 1 h. The antibody-treated membrane was washed with PBS-T several times and incubated with HRP-conjugated antimouse antibody

(1:2500 dilution with 5% skim milk in PBS-T). After being washed with PBS-T several times, Western blotting was performed using an ECL kit (GE Healthcare).

Intracellular Calcium Assay. For calcium signaling analysis, HEK-293 cells expressing hTAS1R2 and hTAS1R3 were cultured for more than 3 days, and 5 μM Fura2-acetoxymethyl (AM) (calcium indicator, Invitrogen) was loaded into the cell in an imaging buffer solution (in mM: NaCl 140, KCl 5, $MgCl_2$ 1, $CaCl_2$ 2, HEPES 10, Glucose 10, 0.1% Pluronic F-127, pH 7.4). After incubation at 37 °C for 30 min, the cells were washed several times with the same buffer solution and incubated for 1 h at 37 °C, so that the AM ester group was cleaved by intracellular esterase. The fluorescence signal upon the addition of sucrose (10 mM) and ATP (100 μM) was measured at 510 nm by dual excitation at 340 and 380 nm using a spectrofluorophotometer (Tecan). The signals were acquired with 2 s intervals. For the calcium imaging analysis of nanovesicles, the nanovesicles containing hTAS1R2 and hTAS1R3 were immobilized on poly-D-lysine-treated 96-well plates by incubation at 37 °C for 2 h. The calcium signal upon the addition of sucrose was measured by the same procedure of calcium signaling analysis for the cells expressing hTAS1R2 and hTAS1R3 described above.

Fabrication of swCNT-FETs. swCNTs (purchased from Hanwha, Korea) were dispersed in 1,2-dichlorobenzene (50 mL) by applying ultrasonic vibration for 20 min. The concentration of swCNT suspensions was 0.05 mg/mL. For swCNT assembly, an octadecyltrichlorosilane self-assembled monolayer with nonpolar terminal groups was first patterned on a SiO_2 (1000 Å) substrate *via* photolithography as reported previously.[15,24,25,30−32] The patterned substrate was placed in the swCNT suspensions for 10 s and rinsed thoroughly with 1,2-dichlorobenzene. In this process, a single layer of swCNTs was selectively adsorbed onto the bare SiO_2 regions. Afterward, contact electrodes were fabricated using conventional photolithography followed by the thermal evaporation of Pd/Au (10 nm/30 nm) and a lift-off process. The gap distance between the source and the drain electrodes was 20 μm. The source and drain electrodes were then passivated with a photoresist (AZ 5214) to avoid leakage currents during the sensing experiments in liquid environments.

Immobilization of Nanovesicles on swCNT Transistors. 1-Pyrenebutanoic acid *N*-hydroxysuccinimidyl ester (PSE, Molecular Probe) solution (1 mM in methanol) was applied onto the fabricated swCNT-FETs for 1 h at room temperature, and the swCNT-FETs were washed three times with fresh methanol. Then, the swCNT-FETs were incubated in the solution including hTAS1R2 and hTAS1R3 expressed nanovesicles for 4 h so that the nanovesicles were selectively attached onto the PSE layer on the swCNT channel region of the swCNT-FETs. In this strategy, the pyrene moieties of PSE molecules interacted with the sidewalls of swCNTs by π-stacking. In addition, succinimidyl groups of the PSE molecules bound to proteins intercalated in the vesicles. As a result, the nanovesicles were successfully integrated with the swCNT-FET devices.

Electrical Measurements. For the sweetener sensing experiment, a NBT was connected to a Keithley 4200 semiconductor analyzer. Then, a 9 μL droplet of DPBS containing 2 mM of $CaCl_2$ at pH 7.4 was placed on the NBT. Source−drain currents were monitored using the semiconductor analyzer while introducing different concentrations of various sweetener solutions. A 100 mV bias voltage was maintained between the source and drain electrodes of the sensor at all times during electrical measurements. For a signal analysis, we employed the relative conductance change (G/G_0) as a sensor signal. Here, the binding of sweeteners to the receptors in the nanovesicles triggered Ca^{2+} influx into nanovesicles, which caused the changes of electrical currents in the underlying swCNT-FET. Thus, we could monitor the activity of hTAS1R2- and hTAS1R3-expressed nanovesicles by measuring the electrical currents.

Preparation of Tastants. Sweeteners used in this study were purchased from Sigma-Aldrich. Tastant solutions were prepared freshly on the day of the experiment. For the coffee solution, DPBS (90 °C) was flowed through a coffee filter by hand drip method, and the solution was cooled to room temperature. For Darjeeling tea, we placed a Darjeeling tea bag into the DPBS (90 °C) for 3 min, and the solution was cooled to room temperature.

Sensory Evaluation. Ninety subjects (40 male, 50 female), ranging in age from 19 to 65 years, were recruited from the Columbus metropolitan area and enrolled in the study with written informed consent under The Ohio State University's Institutional Review Board protocol 2013B0277. Subjects were randomly assigned to 1 of 3 experimental sessions in which they were asked to evaluate the perceived sweet intensity of aspartame (Sigma-Aldrich, St. Louis, MO), sucrose (Giant Eagle, Pittsburgh, PA), or cellobiose (Sigma-Aldrich, St. Louis, MO) solutions and received monetary compensation for participating in the study. Sucrose (0, 7.3×10^{-3}, 14.6×10^{-3}, 29.2×10^{-3}, 0.292, 0.730, and 1.46 M), aspartame (36.5×10^{-6}, 73×10^{-6}, 1.46×10^{-4}, 1.46×10^{-3}, 3.65×10^{-3}, and 7.3×10^{-6} M), and cellobiose (0, 14.6×10^{-3}, 73×10^{-3}, and 0.146 M) solutions were made fresh using deionized water. In each session, subjects ($n = 30$) were presented with solutions from one sweetener series. Solutions were served in 30 mL aliquots in plastic cups (Gordon Food Service, Grand Rapids, MI) at room temperature (21 °C). All sweetener solutions from a given series were presented simultaneously and in random order. Subjects were asked to taste each sample and rank them in order from least sweet to most sweet. To counter the effects of adaptation, subjects were told to rinse with water after tasting each sample. Once sure of their ranking, subjects were then asked to rate the perceived intensity of each solution using the gLMS. Subjects were specifically told that if two samples were perceived as equally sweet (or not sweet), they could give those samples the same ratings. As before, subjects were instructed to rinse with water after tasting each sample. The ranking data were used to improve the precision and accuracy of the ratings and were not further analyzed. Rating data from each experimental session were subjected to analysis of variance (ANOVA) followed by post-hoc Tukey's tests to determine whether perceived sweetness increased with increasing sweetener concentration. Significance was taken at the $p < 0.05$ level. Nonlinear regression was used to fit a concentration−response curve to averaged ratings data from each experimental session. All data are presented as means ± standard error.

Conflict of Interest: The authors declare no competing financial interest.

Acknowledgment. This work was supported by NRF grants (No. 2012-0000144, No. 2012-0006564) and the Converging Research Center Program through the Ministry of Science, ICT & Future Planning, Korea (No. 2012K001365). This work was also supported by the KIST Institutional Program (Project No. 2E24812-14-043). S.H. acknowledges the support from the BioNano Health-Guard Research Center (H-GUARD_2013M3A6B2078961) and the funding programs by the Ministry of Science, ICT & Future Planning (Nos. 2013-007874, 2013M3C8A3078813).

Supporting Information Available: Additional information about production of receptor, fabrication, and stability of the sensor platform. This material is available free of charge *via* the Internet at http://pubs.acs.org.

REFERENCES AND NOTES

1. Luong, J. H. T.; Bouvrette, P.; Male, K. B. Developments and Applications of Biosensors in Food Analysis. *Trends Biotechnol.* **1997**, *15*, 369–377.
2. Terry, L. A.; White, S. F.; Tigwell, L. J. The Application of Biosensors to Fresh Produce and the Wider Food Industry. *J. Agric. Food Chem.* **2005**, *53*, 1309–1316.
3. Habara, M.; Ikezaki, H.; Toko, K. Study of Sweet Taste Evaluation Using Taste Sensor with Lipid/Polymer Membranes. *Biosens. Bioelectron.* **2004**, *19*, 1559–1563.
4. Litvinchuk, S.; Tanaka, H.; Miyatake, T.; Pasini, D.; Tanaka, T.; Bollot, G.; Mareda, J.; Matile, S. Synthetic Pores with Reactive Signal Amplifiers as Artificial Tongues. *Nat. Mater.* **2007**, *6*, 576–580.
5. Riul, A.; dos Santos, D. S.; Wohnrath, K.; Di Tommazo, R.; Carvalho, A. C. P. L. F.; Fonseca, F. J.; Oliveira, O. N.; Taylor,

D. M.; Mattoso, L. H. C. Artificial Taste Sensor: Efficient Combination of Sensors Made from Langmuir–Blodgett Films of Conducting Polymers and a Ruthenium Complex and Self-Assembled Films of an Azobenzene-Containing Polymer. *Langmuir* **2002**, *18*, 239–245.
6. Riul, A.; Malmegrim, R. R.; Fonseca, F. J.; Mattoso, L. H. C. An Artificial Taste Sensor Based on Conducting Polymers. *Biosens. Bioelectron.* **2003**, *18*, 1365–1369.
7. Damak, S.; Rong, M.; Yasumatsu, K.; Kokrashvili, Z.; Varadarajan, V.; Zou, S.; Jiang, P.; Ninomiya, Y.; Margolskee, R. F. Detection of Sweet and Umami Taste in the Absence of Taste Receptor T1r3. *Science* **2003**, *301*, 850–853.
8. Zhao, G. Q.; Zhang, Y.; Hoon, M. A.; Chandrashekar, J.; Erlenbach, I.; Ryba, N. J.; Zuker, C. S. The Receptors for Mammalian Sweet and Umami Taste. *Cell* **2003**, *115*, 255–266.
9. Nelson, G.; Chandrashekar, J.; Hoon, M. A.; Feng, L.; Zhao, G.; Ryba, N. J. P.; Zuker, C. S. An Amino-Acid Taste Receptor. *Nature* **2002**, *416*, 199–202.
10. Nelson, G.; Hoon, M. A.; Chandrashekar, J.; Zhang, Y.; Ryba, N. J. P.; Zuker, C. S. Mammalian Sweet Taste Receptors. *Cell* **2001**, *106*, 381–390.
11. Adler, E.; Hoon, M. A.; Mueller, K. L.; Chandrashekar, J.; Ryba, N. J. P.; Zuker, C. S. A Novel Family of Mammalian Taste Receptors. *Cell* **2000**, *100*, 693–702.
12. Behrens, M.; Brockhoff, A.; Kuhn, C.; Bufe, B.; Winnig, M.; Meyerhof, W. The Human Taste Receptor Htas2r14 Responds to a Variety of Different Bitter Compounds. *Biochem. Biophys. Res. Commun.* **2004**, *319*, 479–485.
13. Mueller, K. L.; Hoon, M. A.; Erlenbach, I.; Chandrashekar, J.; Zuker, C. S.; Ryba, N. J. P. The Receptors and Coding Logic for Bitter Taste. *Nature* **2005**, *434*, 225–229.
14. Song, H. S.; Kwon, O. S.; Lee, S. H.; Park, S. J.; Kim, U.-K.; Jang, J.; Park, T. H. Human Taste Receptor-Functionalized Field Effect Transistor as a Human-like Nanobioelectronic Tongue. *Nano Lett.* **2013**, *13*, 172–178.
15. Kim, T. H.; Song, H. S.; Jin, H. J.; Lee, S. H.; Namgung, S.; Kim, U.-k.; Park, T. H.; Hong, S. "Bioelectronic Super-Taster" Device Based on Taste Receptor–Carbon Nanotube Hybrid Structures. *Lab Chip* **2011**, *11*, 2262–2267.
16. Bockaert, J.; Philippe Pin, J. Molecular Tinkering of G Protein-Coupled Receptors: An Evolutionary Success. *EMBO J.* **1999**, *18*, 1723–1729.
17. Warne, T.; Serrano-Vega, M. J.; Baker, J. G.; Moukhametzianov, R.; Edwards, P. C.; Henderson, R.; Leslie, A. G.; Tate, C. G.; Schertler, G. F. Structure of a B_1-Adrenergic G-Protein-Coupled Receptor. *Nature* **2008**, *454*, 486–491.
18. Lohse, M. J. Dimerization in GPCR Mobility and Signaling. *Curr. Opin. Pharmacol.* **2010**, *10*, 53–58.
19. Milligan, G. G-Protein-Coupled Receptor Heterodimers: Pharmacology, Function and Relevance to Drug Discovery. *Drug Discovery Today* **2006**, *11*, 541–549.
20. Terrillon, S.; Bouvier, M. Roles of G-Protein-Coupled Receptor Dimerization. *EMBO Rep.* **2004**, *5*, 30–34.
21. Albizu, L.; Cottet, M.; Kralikova, M.; Stoev, S.; Seyer, R.; Brabet, I.; Roux, T.; Bazin, H.; Bourrier, E.; Lamarque, L. Time-Resolved FRET between GPCR Ligands Reveals Oligomers in Native Tissues. *Nat. Chem. Biol.* **2010**, *6*, 587–594.
22. Bouvier, M.; Heveker, N.; Jockers, R.; Marullo, S.; Milligan, G. BRET Analysis of GPCR Oligomerization: Newer Does Not Mean Better. *Nat. Methods* **2007**, *4*, 3–4.
23. Maurel, D.; Comps-Agrar, L.; Brock, C.; Rives, M.-L.; Bourrier, E.; Ayoub, M. A.; Bazin, H.; Tinel, N.; Durroux, T.; Prézeau, L. Cell-Surface Protein–Protein Interaction Analysis with Time-Resolved FRET and Snap-Tag Technologies: Application to GPCR Oligomerization. *Nat. Methods* **2008**, *5*, 561–567.
24. Jin, H. J.; Lee, S. H.; Kim, T. H.; Park, J.; Song, H. S.; Park, T. H.; Hong, S. Nanovesicle-Based Bioelectronic Nose Platform Mimicking Human Olfactory Signal Transduction. *Biosens. Bioelectron.* **2012**, *35*, 335–341.
25. Park, J.; Lim, J. H.; Jin, H. J.; Namgung, S.; Lee, S. H.; Park, T. H.; Hong, S. A. Bioelectronic Sensor Based on Canine Olfactory Nanovesicle–Carbon Nanotube Hybrid Structures for the Fast Assessment of Food Quality. *Analyst* **2012**, *137*, 3249–3254.
26. Karachevtsev, V. A.; Stepanian, S. G.; Glamazda, A. Y.; Karachevtsev, M. V.; Eremenko, V. V.; Lytvyn, O. S.; Adamowicz, L. Noncovalent Interaction of Single-Walled Carbon Nanotubes with 1-Pyrenebutanoic Acid Succinimide Ester and Glucoseoxidase. *J. Phys. Chem. C* **2011**, *115*, 21072–21082.
27. Salahpour, A.; Bonin, H.; Bhalla, S.; Petäjä-Repo, U.; Bouvier, M. Biochemical Characterization of B2-Adrenergic Receptor Dimers and Oligomers. *Biol. Chem.* **2003**, *384*, 117–123.
28. Dong, H.; Dunn, J.; Lytton, J. Stoichiometry of the Cardiac Na^+/Ca^{2+} Exchanger Ncx1.1 Measured in Transfected HEK Cells. *Biophys. J.* **2002**, *82*, 1943–1952.
29. Liu, M.; Chen, T.-Y.; Ahamed, B.; Li, J.; Yau, K.-W. Calcium–Calmodulin Modulation of the Olfactory Cyclic Nucleotide-Gated Cation Channel. *Science* **1994**, *266*, 1348–1354.
30. Kim, T. H.; Lee, S. H.; Lee, J.; Song, H. S.; Oh, E. H.; Park, T. H.; Hong, S. Single-Carbon-Atomic-Resolution Detection of Odorant Molecules Using a Human Olfactory Receptor-Based Bioelectronic Nose. *Adv. Mater.* **2009**, *21*, 91–94.
31. Lee, S. H.; Jin, H. J.; Song, H. S.; Hong, S.; Park, T. H. Bioelectronic Nose with High Sensitivity and Selectivity Using Chemically Functionalized Carbon Nanotube Combined with Human Olfactory Receptor. *J. Biotechnol.* **2012**, *157*, 467–472.
32. Lim, J. H.; Park, J.; Oh, E. H.; Ko, H. J.; Hong, S.; Park, T. H. Nanovesicle-Based Bioelectronic Nose for the Diagnosis of Lung Cancer from Human Blood. *Adv. Healthcare Mater.* **2014**, *3*, 360–366.
33. Li, X.; Staszewski, L.; Xu, H.; Durick, K.; Zoller, M.; Adler, E. Human Receptors for Sweet and Umami Taste. *Proc. Natl. Acad. Sci. U.S.A.* **2002**, *99*, 4692–4696.
34. Christensen, S. M.; Stamou, D. G. Sensing-Applications of Surface-Based Single Vesicle Arrays. *Sensors* **2010**, *10*, 11352–11368.
35. Ciosek, P.; Wróblewski, W. Sensor Arrays for Liquid Sensing–Electronic Tongue Systems. *Analyst* **2007**, *132*, 963–978.
36. Sehra, G.; Cole, M.; Gardner, J. W. Miniature Taste Sensing System Based on Dual SH-SAW Sensor Device: An Electronic Tongue. *Sens. Actuators, B* **2004**, *103*, 233–239.
37. Winquist, F.; Wide, P.; Lundström, I. An Electronic Tongue Based on Voltammetry. *Anal. Chim. Acta* **1997**, *357*, 21–31.